A Projection Transformation Method for Eliminating Crosstalk in Networked Thermopile Arrays

Wanjin Feng, Jianyu Fu, Ying Hou, Chao Liu, Peng Huang, and Dapeng Chen

***Abstract*—The networked thermopile array in row-column fashion suffered from the crosstalk caused by parasitic parallel paths. To measure accurate two-dimensional thermal information, it is of great importance to eliminate the crosstalk. In this work, based on the response voltage non-linearity of thermopile pixels as well as the response voltage non-uniformity of array, a projection transformation method that suits for small-scale networked thermopile arrays is proposed. It transforms the crosstalk elimination problem into an overdetermined non-linear least squares problem, and is solved by the Newton-Raphson iterative algorithm. Its reconstruction error is analyzed carefully by Monte Carlo simulation, and its ability to implement non-uniformity and defective pixel correction is also discussed. Its validity is verified experimentally using a 3 × 3 networked thermopile array. The experimental result shows that the original IR image can be reconstructed from measured IR images by this method, and the reconstruction error is significantly decreased from 17.03% to 2.10%.**

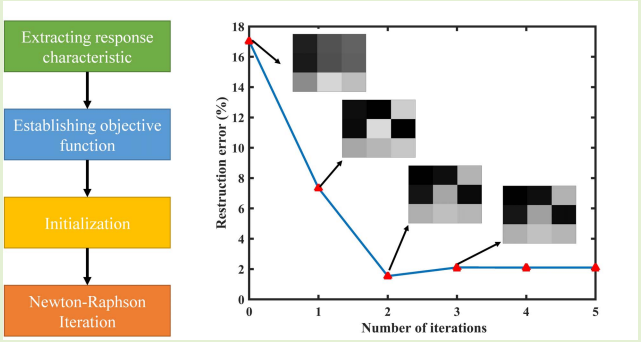

***Index Terms*—Crosstalk elimination, projection transformation, networked thermopile arrays, Newton-Raphson iterative algorithm, non-linear least squares.**

I. Introduction

THERMOPILE sensors utilize the Seebeck effect to generate an electric signal in proportion to the physical phenomena that need to be measured [1]. They have advantages of no electric excitation, negligible 1/f noise and low power consumption [2]–[4]. There are basically two kinds of thermopile sensors classified by the pixel number: the single and multi-pixel thermopile sensors. The single-pixel thermopile sensors have been studied extensively, and they are widely used in infrared (IR) radiation detection, gas sensing, vacuum measurement, *etc*. [5]–[7].

The multi-pixel thermopile sensors, that is, thermopile arrays could detect two-dimensional thermal information, so they draw considerable attention in recent years [8]–[11]. Each pixel in arrays has two ends. As the size of arrays increases, networked arrangement is introduced [12]. The shared rows and columns make the outputs of a $M \times N$ thermopile array reduce from $2 \times M \times N$ to $M + N$. This is very helpful in reducing the interconnection complexity, however, the crosstalk from parasitic parallel paths inevitably exists [13]. Hou *et al.* had investigated the electrical equivalent circuit of networked thermopile arrays, and set up its mathematical model. Theory analysis showed that the actual response voltages of pixels cannot be solved directly because there are only $M + N - 1$ effective equations of a $M \times N$ thermopile array [14]. In this case, eliminating the crosstalk in networked thermopile arrays is of great importance.

Networked resistive arrays face the same problem. Three main approaches have been proposed. One is adding peripheral controller, which limits the port voltages of non-scanned pixels (NSPs) in the array. Wu *et al.* proposed the voltage feedback method. The bypass currents on NSPs are restrained with output voltage feeding back to column and row wires

Manuscript received November 23, 2021; revised December 26, 2021; accepted December 27, 2021. Date of publication December 28, 2021; date of current version February 11, 2022. This work was supported in part by the National Natural Science Foundation of China under Grant 61601455 and Grant 61874137 and in part by the Scientific Instrument Developing Project of the Chinese Academy of Sciences under Grant ZDKYYQ20200007. The associate editor coordinating the review of this article and approving it for publication was Dr. Joseph Shor. *(Corresponding author: Jianyu Fu.)*

Wanjin Feng, Chao Liu, and Peng Huang are with the Key Laboratory of Microelectronic Device and Integrated Technology, Institute of Microelectronics, Chinese Academy of Sciences, Beijing 100029, China, and also with the School of Microelectronics, University of Chinese Academy of Sciences, Beijing 100049, China.

Jianyu Fu, Ying Hou, and Dapeng Chen are with the Key Laboratory of Microelectronic Device and Integrated Technology, Institute of Microelectronics, Chinese Academy of Sciences, Beijing 100029, China, also with the University of Chinese Academy of Sciences, Beijing 100049, China, and also with Wuxi IoT Innovation Center Company Ltd., Wuxi, Jiangsu 214135, China (e-mail: fujianyu@ime.ac.cn).

Digital Object Identifier 10.1109/JSEN.2021.3139081

through an op-amp [15], [16]. Lazzarini *et al.* presented zero potential method. All driving-electrodes of NSPs have zero potential by connected to virtual ground with driving op-amps [17]. This approach is not suitable for networked thermopile arrays because each thermopile pixel could generate voltage itself. Therefore, the crosstalk currents cannot be eradicated and the scanned pixel (SP) will still be affected even in the case of limiting the port voltages of NSPs.

Another is establishing and solving resistance matrix equations to obtain each pixel's resistance. By changing the port voltages or currents of networked resistive arrays, matrix equations are well-posed. Lin *et al.* proposed resistance matrix method. It takes advantage of the microcontroller in sensor scanning to establish resistance matrix equations [18]. Federico *et al.* proposed incidence matrix method. It estimates the internal resistance distribution by taking injected current from the current source [19]. However, on account of superposition theorem, changing the port voltages or currents cannot add effective equations of response voltages, so matrix equations are still ill-posed for networked thermopile arrays.

The other is using switch to separate SP from its parasitic parallel paths. Snyder *et al.* and Someya *et al.* used diodes and transistors separately to block the parasitic parallel currents on NSPs [20], [21]. It could be applied to networked thermopile arrays, and MOS transistors have been used by Heimann and Melexis [22]. However, MOS transistors will increase both the challenges of design and manufacture. In addition, it also will introduce measurement deviation due to the transistor's discrete drain-source voltage [13].

In this work, a projection transformation method that aims for small-scale array is proposed. It is based on the response voltage non-linearity of thermopile pixels as well as the response voltage non-uniformity of array. The structure and working principle of networked thermopile array is firstly analyzed. Then, the crosstalk elimination problem is transformed into a non-linear least squares problem and its objective function is derived. After that, the projection transformation method is presented, and the reconstruction error is evaluated by Monte Carlo simulation. Moreover, its benefits in non-uniformity and defective pixel correction are explored. Finally, the application of this method to a 3×3 thermopile array is described.

II. Structure and Principle

A. Thermopile Pixel

The schematic view of a thermopile pixel is shown in Fig. 1. It consists of a sensitive region, a substrate, a framework, and supporting legs. The framework is fixed on substrate. The sensitive region, which is suspended over substrate, is connected to framework by supporting legs. Several thermocouple pairs in series are imbedded in supporting legs. And their hot and cold junctions are located in sensitive region and framework, respectively. According to the Seebeck effect, thermoelectric voltage is generated when there is a temperature difference between sensitive region and framework.

Taking IR detection as an example, the incident IR radiation is absorbed by sensitive region and makes a temperature rise in this region. The temperature difference between sensitive region and framework can be given by [23]:

$$T_{diff} = T_h - T_c = \frac{\eta p_0}{G_{total}} \tag{1}$$

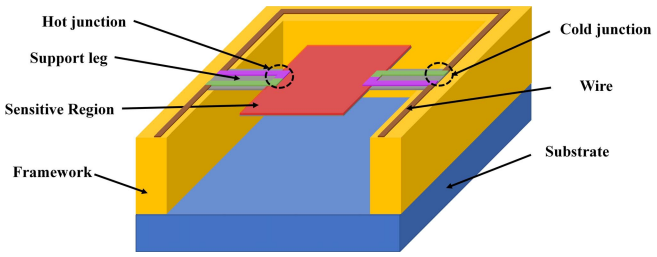

Fig. 1. Schematic view of a thermopile pixel.

where T_h and T_c are separately the temperature of sensitive region and framework, η is the IR absorptance of sensitive region, p_0 is the incident IR radiation power, and G_{total} is the total thermal conductance of thermopile pixel.

The response voltage ΔV generated by thermopile can be described mathematically as [23]:

$$\Delta V = N_{cp} \alpha_{AB} T_{diff} \tag{2}$$

where N_{cp} is the number of thermocouples, α_A and α_B are the Seebeck coefficients of two thermoelectric material that used in thermocouples, and their difference is α_{AB}.

By combining (1) and (2), the response voltage can be expressed as:

$$\Delta V = \frac{N_{cp} \eta \alpha_{AB}}{G_{total}} p_0 = R p_0 \tag{3}$$

where R is the responsivity of thermopile pixel.

For one thing, there is non-linear relationship between the incident IR radiation power p_0 and the radiation temperature T of the object to be measured according to the law of thermal radiation energy transfer [24], [25]. This further leads to the non-linear response voltage of thermopile pixels to the radiation temperature.

For another thing, the fabrication non-uniformity will generally induce non-uniformity of Seebeck coefficient and total thermal conductance of thermopile pixels. The non-uniformity can be evaluated by coefficient of variation. The response voltage non-uniformity is positively associated with non-uniformity of both Seebeck coefficient and total thermal conductance.

B. Networked Thermopile Array

A thermopile pixel can be equivalent to a resistor in series with a voltage source, and a schematic view of a networked thermopile array is shown in Fig. 2. The two ends of each thermopile pixel are separately connected to the column line and row line. The response voltage and output voltage of pixel in the row i and column j are denoted as $\Delta V_{i,j}$ and $V_{i,j}$, respectively.

As an unknown IR radiation radiates the networked thermopile array, the response voltages can be expressed by the radiation temperature $T = [T_{ij}]_{M \times N}$, which be approximately fitted by a quadratic function:

$$\Delta V = f(T) = a * T * T + b * T + c \tag{4}$$

where $\Delta V = [\Delta V_{ij}]_{M \times N}$, $\Delta V_{ij} = f_{ij}(T_{ij})$, $*$ is element-wise product and $a = [a_{ij}]_{M \times N}$, $b = [b_{ij}]_{M \times N}$, $c = [c_{ij}]_{M \times N}$. The equation is non-linear due to the response voltage non-linearity of thermopile pixels.

The relationship between response voltages ΔV and output voltages V of each pixel can be derived by Kirchhoff's current

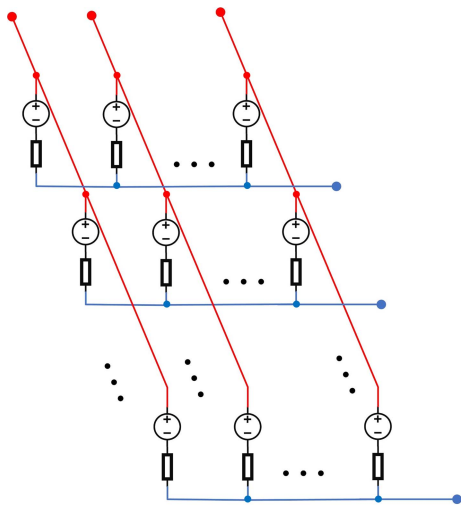

Fig. 2. Schematic view of a networked $M \times N$ thermopile array.

and voltage laws [14]:

$$\begin{bmatrix} D \\ O \end{bmatrix} vec(\Delta V) = \begin{bmatrix} D \\ F \end{bmatrix} vec(V) \tag{5}$$

where D and F are coefficient matrixes that represent all lines and all independent closed loops in the networked thermopile array, respectively. O is a zero matrix.

To reconstruct the unknown IR radiation, let:

$$X = vec(T) \tag{6}$$

$$S(X) = Dvec(\Delta V) = Dvec(f(T)) \tag{7}$$

$$U = Dvec(V) \tag{8}$$

Then:

$$S(X) = U = U_0 + W \tag{9}$$

where $S(X)$ is the non-linear signal model related to the unknown IR radiation X, U is the data vector related to output voltages V, U_0 and W are noise-free data vector and noise vector, respectively.

The crosstalk elimination problem can be transformed into a non-linear least squares problem. Its objective function is:

$$\min_X J = W^2 = (U - S(X))^T (U - S(X)) \tag{10}$$

The unknown IR radiation cannot be directly reconstructed because of the underdetermined characteristic.

III. Projection Transformation Method

A. Extracting Response Characteristic

According to (4), it is necessary to get response characteristics of pixels before reconstructing unknown IR radiation. The fitting parameters are taken as an uncertain response characteristic P:

$$P = \begin{bmatrix} vec(a)^T & vec(b)^T & vec(c)^T \end{bmatrix} \tag{11}$$

Let:

$$\Gamma_T = \begin{bmatrix} vec([\,T * T & T & I_{M\times N}\,])^T \\ \vdots \\ vec([\,T * T & T & I_{M\times N}\,])^T \end{bmatrix}_{(M+N-1)\times(3MN)} \tag{12}$$

where $I_{M\times N}$ is a $M \times N$ all-ones matrix.

By combining (4), (11) and (12), there is:

$$\begin{bmatrix} D & D & D \end{bmatrix} * \Gamma_T P = Dvec(V) \tag{13}$$

It is known that the response voltage of each thermopile pixel is 0 at ambient radiation temperature T_0, and can be expressed as:

$$vec(f(T_0)) = O_{MN\times 1} \tag{14}$$

To solve the uncertain response characteristic P, additional L_P sets of (13) should be constructed by using different radiation temperature to radiate pixels. The radiation temperatures are as different and irregular as possible. And L_P must satisfy the following condition:

$$L_p \times (M + N - 1) > 2 \times M \times N \tag{15}$$

Therefore, an overdetermined system of linear equations can be established using (13) and (14):

$$H_p P = Q \tag{16}$$

where H_P is a coefficient matrix related to both radiation temperatures and ambient temperature, and its rank$(H_P) = 3MN$, Q is a data vector related to output voltages. Using least squares method to solve (16), we can get:

$$P = (H_P^T H_P)^{-1} H_P^T Q \tag{17}$$

B. Operation Principle

Different pixels will respond differently under a same IR radiation as a result of the response voltage non-uniformity of array. Therefore, transforming the projection of IR radiation on array can set up additional (9) under the same unknown IR radiation. Assuming the operation number of projection transformation is $L - 1$, it must be satisfied:

$$L \times (M + N - 1) > M \times N \tag{18}$$

On this condition, the underdetermined non-linear least squares problem is converted into an overdetermined non-linear least squares problem.

There are many ways to realize transforming the projection of IR radiation such as, rotation, translation, occlusion, as shown in Fig. 3. Rotating and translating the thermopile array can be realized through machinery, and occlusion can be realized by a shutter.

C. Newton-Raphson Iterative Algorithm

After the projection transformation, $L \times M \times N$ equations based on (9) are set up. To solve the overdetermined non-linear least squares problem, Newton-Raphson iterative algorithm [26] is used as follows:

Step 1: Solve (4) by taking output voltages as response voltages to obtain the initial crosstalk solution $X_{i=0} = vec(T_{i=0})$.

Step 2: Use Taylor expansion to get the first-order approximation of $S(X_i)$ in the neighborhood of current solution X_i, which is:

$$S(X_i) = H_i X_i + C_i \tag{19}$$

Then, (9) can be derived as:

$$H_i X_i = U - C_i \tag{20}$$

where H_i is the coefficient matrix which size is $L(M + N) \times MN$, and rank$(H_i) = 3MN$.

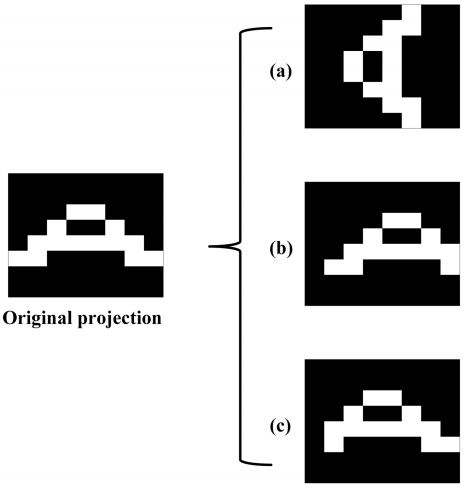

Fig. 3. Schematic diagram of projection transformation method. (a) rotated projection, (b) translational projection, (c) occluded projection.

Step 3: Use the least squares method to solve (20), and get:

$$X_{i+1} = (H_i^T H_i)^{-1} H_i^T (U - C_i) \tag{21}$$

Step 4: If the stop condition $|X_{i+1} - X_i| \leq \varepsilon$ holds, stop the iteration; Otherwise, set $i = i + 1$, go to **Step 2**. And ε is the minimum iteration step size set by the algorithm.

IV. Analysis

A. Reconstruction Error

The noise of output voltages, which is caused by Johnson noise, shot noise, temperature fluctuation noise, etc., will affect the reconstruction error. To evaluate the noise, the noise-to-signal ratio (NSR) is defined as:

$$NSR = \frac{\sigma_N}{A_O} \times 100\% \tag{22}$$

where σ_N and A_O are separately the standard deviation of noise and the output voltage amplitude.

Fig. 4 shows the comparison of original IR image, simulated output IR image, and reconstructed IR image (3 projection rotation operations) under the conditions that non-uniformity of response voltages is 5% and NSR = 0.5%. When response characteristic P is known, output voltages V of a 5×5 thermopile array can be obtained by calculating (4) and (5), and the simulated output IR image is further acquired by substituting V into (4) [14]. It can be seen from Fig. 4 (b) that the diagonal line is completely disappeared in the simulated output IR image because of crosstalk currents from parasitic parallel paths. However, it could be restored by projection transformation method as shown in Fig. 4 (c), and the difference between original and reconstructed IR images, which is caused by noise is small.

Under the above-mentioned conditions, Fig. 5 illustrates the simulated relation of reconstruction error (mean absolute percentage error, MAPE) to array size and NSR using Monte Carlo simulation (10000 samples). In this figure, the reconstruction error increases with increasing NSR and array size. With array size increasing, the number of effective equations does not increase as fast as the number of unknown variables that induces a lager condition number cond(H_i) in the iterative algorithm. And it means the solution X is more sensitive to noise [27], [28]. Larger-scale arrays need more transformation operations to build more effective equations for achieving the same effect as small-scale arrays. Therefore, projection transformation method is more suitable for small-scale arrays. An interesting result can be seen from this figure that MAPE = 0 when NSR = 0. This indicates that the crosstalk can be completely eliminated by projection transformation method in the absence of noise.

Fig. 6 reveals the simulated relationship between the reconstruction error and the response voltage non-uniformity of array under the conditions that array size is 5×5 and NSR = 1%. The reconstruction error is approximately

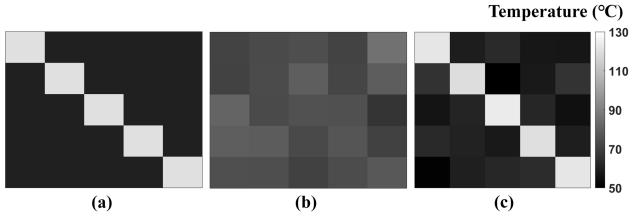

Fig. 4. Comparison of (a) original IR image, (b) simulated output IR image, and (c) reconstructed IR image.

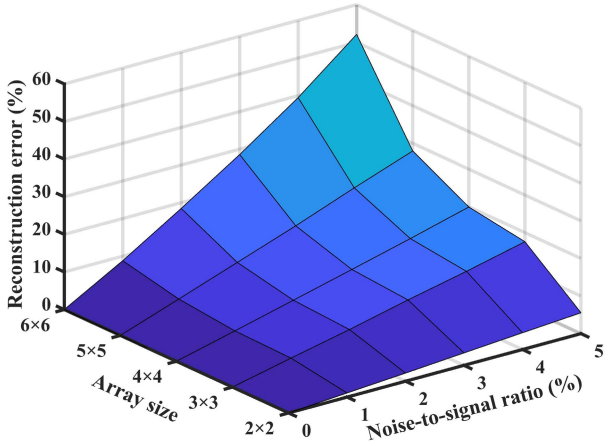

Fig. 5. Simulated relation of reconstruction error to array size and NSR.

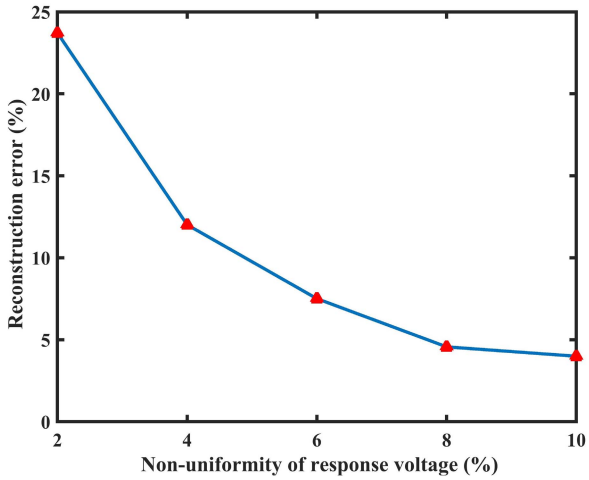

Fig. 6. Simulated relationship between the reconstruction error and the response voltage non-uniformity of array.

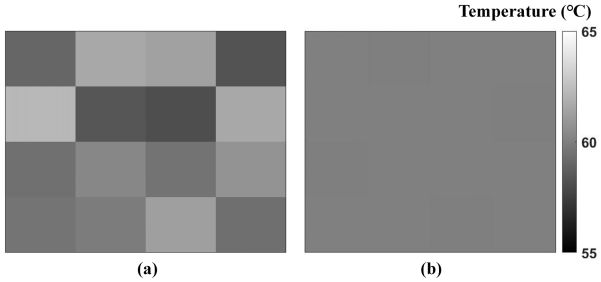

Fig. 7. Non-uniformity correction. (a) original IR image, and (b) reconstructed IR image.

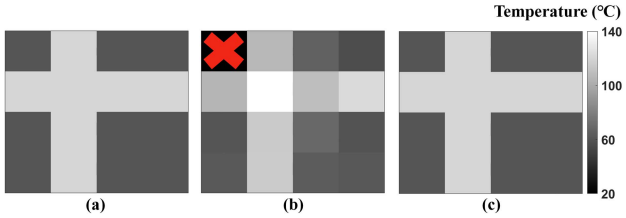

Fig. 8. Defective pixel correction. (a) original IR image, (b) simulated output IR image, (c) reconstructed IR image.

inversely proportional to the response voltages non-uniformity. The more non-uniform the response voltages are, the lower the sensitivity of reconstructed IR image to noise is. This is as a result of smaller condition number in iterative algorithm [29].

Above analysis confirms that the reconstruction error of this method is determined by array size, NSR and non-uniformity of response voltages. Under the conditions that non-uniformity of response voltages is 5% (6.7% in [14]) and NSR = 1% (signal-to-noise ratio of images is typically no less than 40 dB [30]), this method is recommended for small-scale arrays with an array size of 6 × 6 or less to avoid the reconstruction error greater than 10%. However, it could be applied to a lager array, if NSR is smaller than 1% or more projection transformation operations are taken.

B. Features

Traditionally, the response voltage non-uniformity of array is considered as fixed pattern noise that distorts the IR image. Fig. 7 shows the original and reconstructed IR image at a uniform IR radiation temperature (60 °C) by simulation under the condition that non-uniformity of response voltages is 5%. It can be seen that the IR image could be more uniform by using projection transformation method because it takes advantage of non-uniformity of response voltages to solve IR radiation temperatures of pixels. This demonstrates that this method has ability to correct the non-uniformity of array.

There are always defective pixels in array. The defective pixels are those either do not work or whose parameters vary greatly from design value [31]. Fig. 8 compares the original IR image, simulated output IR image, and reconstructed IR image. In Fig. 8 (b), a defective pixel which response voltage is always 0 V at any radiation temperature exists in the first row and first column. Since the defective pixel is replaced with normal pixels during projection transformation, the incident radiation on the defective pixel could be completely restored as shown in Fig. 8 (c). Hence, by using projection transformation method, the subsequent image processing algorithm could be greatly simplified.

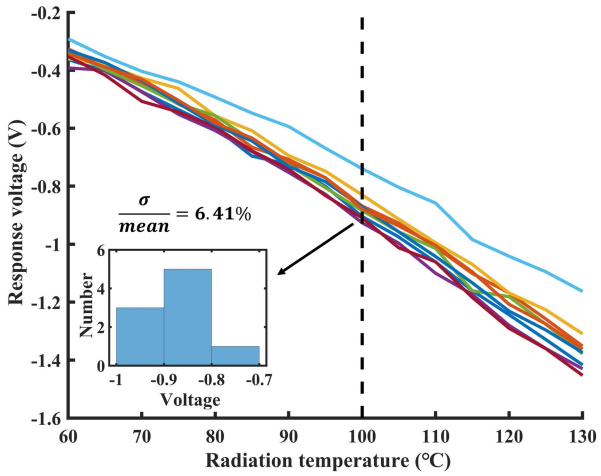

Fig. 9. Response voltages non-uniformity of IR thermopile detectors.

V. Experiment

In order to demonstrate experimentally the effectiveness of proposed projection transformation method, 9 IR thermopile detectors (HINOVAIC W-TRS-5.5), which are single-pixel thermopile sensors, are used. Fig. 9 shows the response voltages of array measured using blackbody source (ELETRIP BR500) and digital oscilloscope (Agilent MSO-X2022A). The ambient temperature is 20 °C, and IR radiation ranges from 60 °C to 130 °C with 10 °C increment each time. It can be seen that the response voltages and their difference increase with the increase of IR radiation temperature, and the non-uniformity is 6.41% at 100 °C. This is due to the fact that the detectors response non-linearity is more obvious when the temperate difference T_{diff} is larger.

A 3 × 3 thermopile array is constructed by these detectors. Fig. 10 shows the schematic view of test setup. Two interconnected subarrays constitute a networked thermopile array in the electrical sense, although they are physically separated. Each subarray is irradiated by a blackbody source spaced 5 cm apart. Different IR images can be achieved by changing the positions of detectors and the temperatures of two blackbody sources. The array automatically addressed by a multiplexer (MUX, ADI ADG712). The output voltages of each detector under IR radiation are amplified 125 times by an amplifier (ADI AD8551) and digitized by an ADC (ADI AD9240), and then saved in a personal computer (PC). All the process is controlled by a field-programmable gate array (FPGA, Terasic DE10-Standard). Finally, according to their pixel positions, the IR images are obtained by calculating output voltages of corresponding detectors by MATLAB on PC.

The array is irradiated by 20 different IR radiations which range from 60 °C to 130 °C, and the response characteristic of each detector is obtained by (17). Fig. 11 compares response voltages and response characteristic curves of 3 IR thermopile detectors. It can be seen that the response characteristic curves pass through most corresponding actual data points and play a similar role to data fitting.

Fig. 12 shows an IR image imaged by this 3 × 3 thermopile array. Fig. 12 (b) shows the measured IR images obtained

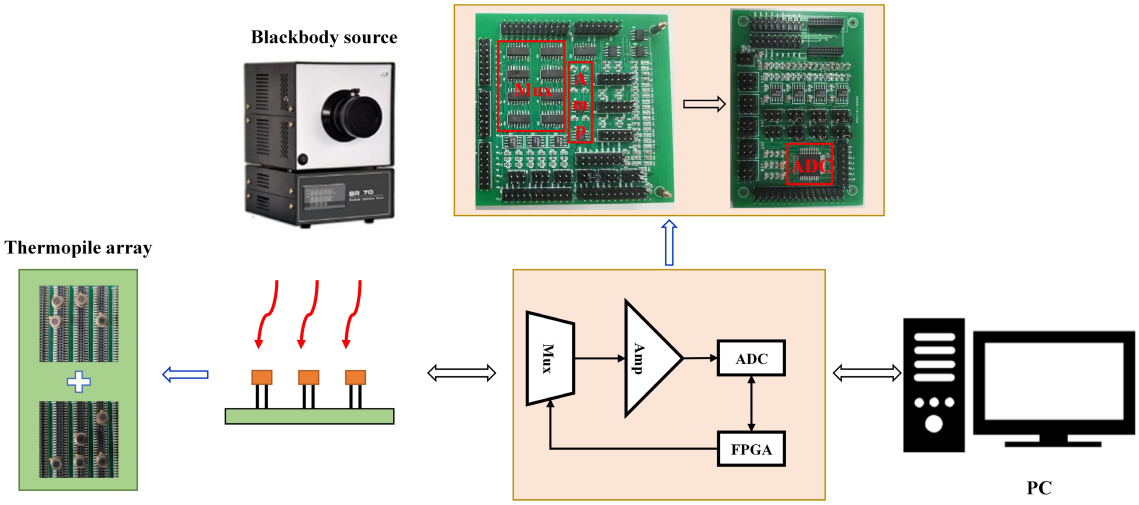

Fig. 10. A 3 × 3 thermopile array and its testing setup.

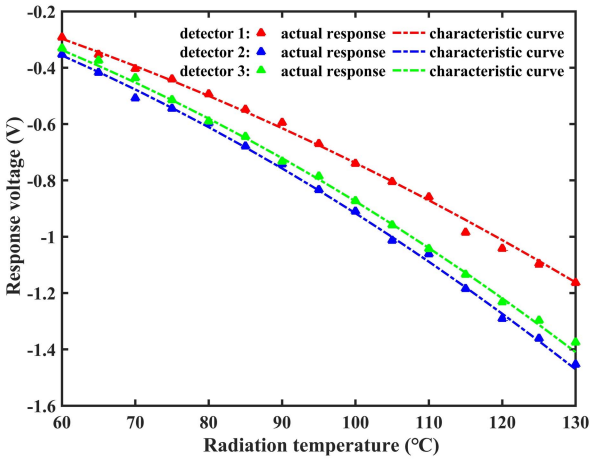

Fig. 11. Actual response voltages and response characteristic curves of 3 IR thermopile detectors.

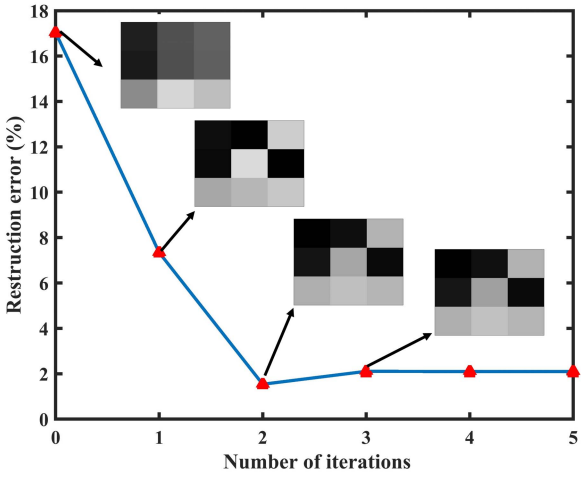

Fig. 13. Error curve with the number of iterations.

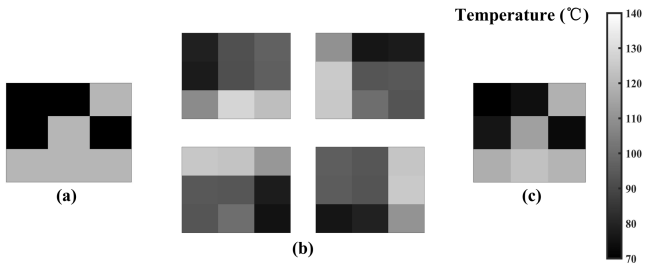

Fig. 12. Crosstalk elimination effect diagram. (a) original IR image, (b) measured IR images got by rotation operation, (c) reconstruction IR image.

through 3 projection rotation operations, and each rotation is 90 degrees. It can be seen that the measured IR images are distorted by crosstalk. And after crosstalk elimination, the reconstruction IR image is basically the same as original IR image. The reconstruction error of IR images before and after crosstalk elimination are separately 17.03% and 2.10% under NSR ≈ 1%.

Fig. 13 shows the relationship between the reconstructing error of thermopile array and the number of iterations. It can be seen that the algorithm reaches a stable solution in the third generation, which means the algorithm can converge quickly. This is because according to (12) and (13), the objective function is actually a quartic function.

VI. Conclusion

A projection transformation method for eliminating the crosstalk in small-scale networked thermopile arrays is proposed. This method is based on the response voltage non-linearity of thermopile pixels as well as the response voltage non-uniformity of array, and could be realized by simple mechanical operations on the array. The mechanical operations can be further replaced by image matching between subsequent frames in dynamic imaging. It has the advantage of being able to correct non-uniformity and defective pixel. The effectiveness of this method is demonstrated by using a 3 × 3 thermopile array. In our experiment, the original IR image is restored from crosstalk IR images, and the reconstruction error of IR image is decreased from 17.03% to 2.10%. The reconstruction error can be further reduced by using application specific integrated circuit and taking more projection transformation operations. The presented method is

easy to apply as no changes made to networked thermopile arrays. It is suitable for small-scale arrays with an array size of 6×6 or less to avoid the reconstruction error greater than 10%, under the conditions that non-uniformity of response voltages is 5% and NSR = 1%. And it can be used for a larger array by decreasing NSR or taking more projection transformation operations. To further extend this method to larger-scale networked thermopile arrays we will represent a detailed method that utilizes the transient response voltage non-uniformity of arrays in a forthcoming paper.

REFERENCES

[1] Y. Wang *et al.*, "First-principles thermodynamic theory of Seebeck coefficients," *Phys. Rev. B, Condens. Matter*, vol. 98, no. 22, Dec. 2018, Art. no. 224101.

[2] D. Popa, S. Z. Ali, R. Hopper, Y. Dai, and F. Udrea, "Smart CMOS mid-infrared sensor array," *Opt. Lett.*, vol. 44, no. 17, pp. 4111–4114, Sep. 2019.

[3] M. C. Foote *et al.*, "Thermopile detector arrays for space science applications," *Proc. SPIE*, vol. 4999, pp. 443–447, 2003.

[4] W. Li, Z. Ni, J. Wang, and X. Li, "A front-side microfabricated tiny-size thermopile infrared detector with high sensitivity and fast response," *IEEE Trans. Electron Devices*, vol. 66, no. 5, pp. 2230–2237, May 2019.

[5] K. Wang *et al.*, "Thermopile infrared detector with detectivity greater than 10 8 cmHz (1/2)/W," *J. Infr., Millim., THz Waves*, vol. 31, no. 7, pp. 810–820, 2010.

[6] L. Houlet *et al.*, "Thermopile sensor-devices for the catalytic detection of hydrogen gas," *Sens. Actuators B, Chem.*, vol. 130, no. 1, pp. 200–206, Mar. 2008.

[7] S.-J. Chen and Y.-C. Wu, "Active thermoelectric vacuum sensor based on frequency modulation," *Micromachines*, vol. 11, no. 1, p. 15, Dec. 2019.

[8] A. D. Shetty, B. Shubha, and K. Suryanarayana, "Detection and tracking of a human using the infrared thermopile array sensor—'Grid-EYE,"' in *Proc. Int. Conf. Intell. Comput., Instrum. Control Technol. (ICICICT)*, Jul. 2017, pp. 1490–1495.

[9] R. Rubio *et al.*, "Non-selective NDIR array for gas detection," *Sens. Actuators B, Chem.*, vol. 127, no. 1, pp. 69–73, Oct. 2007.

[10] G. Sun, T. Saga, T. Shimizu, Y. Hakozaki, and T. Matsui, "Fever screening of seasonal influenza patients using a cost-effective thermopile array with small pixels for close-range thermometry," *Int. J. Infectious Diseases*, vol. 25, pp. 56–58, Aug. 2014.

[11] Y. Zhang and B. Yang, "Traffic flow detection using thermopile array sensor," *IEEE Sensors J.*, vol. 20, no. 10, pp. 5155–5164, May 2020.

[12] A. D. Shetty and G. Toney, "Detection of intruders in warehouses using infrared based thermopile sensor array," *IOP Conf. Ser., Mater. Sci. Eng.*, vol. 376, Jun. 2018, Art. no. 012087.

[13] J. F. Wu, "Scanning approaches of 2-D resistive sensor arrays: A review," *IEEE Sensors J.*, vol. 17, no. 4, pp. 914–925, Feb. 2017.

[14] Y. Hou *et al.*, "Analysis of crosstalk effect in multi-pixel thermopile sensors with networked arrangement," *IEEE Sensors J.*, vol. 21, no. 12, pp. 13350–13355, Jun. 2021.

[15] J. Wu, L. Wang, and J. Li, "Design and crosstalk error analysis of the circuit for the 2-D networked resistive sensor array," *IEEE Sensors J.*, vol. 15, no. 2, pp. 1020–1026, Feb. 2015.

[16] J. Wu, L. Wang, J. Li, and A. Song, "A novel crosstalk suppression method of the 2-D networked resistive sensor array," *Sensors*, vol. 14, no. 7, pp. 12816–12827, 2014.

[17] R. Lazzarini, R. Magni, and P. Dario, "A tactile array sensor layered in an artificial skin," in *Proc. IEEE/RSJ Int. Conf. Intell. Robots Syst.*, vol. 3, Aug. 1995, pp. 114–119.

[18] L. Shu, X. Tao, and D. D. Feng, "A new approach for readout of resistive sensor arrays for wearable electronic applications," *IEEE Sensors J.*, vol. 15, no. 1, pp. 442–452, Jan. 2015.

[19] F. Lorussi, W. Rocchia, E. P. Scilingo, A. Tognetti, and D. D. Rossi, "Wearable, redundant fabric-based sensor arrays for reconstruction of body segment posture," *IEEE Sensors J.*, vol. 4, no. 6, pp. 807–818, Dec. 2004.

[20] W. E. Snyder and J. S. Clair, "Conductive elastomers as sensor for industrial parts handling equipment," *IEEE Trans. Instrum. Meas.*, vol. IM-27, no. 1, pp. 94–99, Mar. 1978.

[21] T. Someya, T. Sekitani, S. Iba, Y. Kato, H. Kawaguchi, and T. Sakurai, "A large-area, flexible pressure sensor matrix with organic field-effect transistors for artificial skin applications," *Proc. Nat. Acad. Sci. USA*, vol. 101, no. 27, pp. 9966–9970, 2004.

[22] M. Kimata, "Uncooled infrared focal plane arrays," *IEEJ Trans. Electr. Electron. Eng.*, vol. 13, no. 1, pp. 4–12, 2017.

[23] C. Escriba, E. Campo, D. Estève, and J. Y. Fourniols, "Complete analytical modeling and analysis of micromachined thermoelectric uncooled IR sensors," *Sens. Actuators A, Phys.*, vol. 120, no. 1, pp. 267–276, 2005.

[24] E. G. Cravalho, C. L. Tien, and R. P. Caren, "Effect of small spacing on radiative transfer between two dielectrics," *J. Heat Transf., Trans. ASME, C*, vol. 89, pp. 351–358, Nov. 1967.

[25] K. Lapworth, T. Quinn, and L. Allnutt, "A black-body source of radiation covering a wavelength range from the ultraviolet to the infrared," *J. Phys. E, Sci. Instrum.*, vol. 3, no. 2, p. 116, 1970.

[26] S. M. Kay and S. M. Kay, *Fundamentals of Statistical Signal Processing: Estimation Theory*. Englewood Cliffs, NJ, USA: Prentice-Hall, 1993.

[27] A. Pyzara, B. Bylina, and J. Bylina, "The influence of a matrix condition number on iterative methods' convergence," in *Proc. Federated Conf. Comput. Sci. Inf. Syst. (FedCSIS)*, Sep. 2011, pp. 459–464.

[28] A. K. Cline, C. B. Moler, G. W. Stewart, and J. H. Wilkinson, "An estimate for the condition number of a matrix," *SIAM J. Numer. Anal.*, vol. 16, no. 2, pp. 368–375, 1979.

[29] H. Dudek, "The relationship between a condition number and coefficients of variation," *Przegląd Statystyczny*, vol. 1, no. 52, pp. 75–85, 2005.

[30] Q. Zhang and R. Ward, "Automatic assessment of signal-to-thermal noise ratio of television images," *IEEE Trans. Consum. Electron.*, vol. 41, no. 1, pp. 108–117, Feb. 1995.

[31] W. Isoz, T. Svensson, and I. Renhorn, "Nonuniformity correction of infrared focal plane arrays," *Proc. SPIE*, vol. 5783, pp. 949–960, May 2005.

Wanjin Feng received the B.S. degree from the Wuhan University of Technology in 2019. He is currently pursuing the master's degree with the Institute of Microelectronics, Chinese Academy of Sciences.

Jianyu Fu received the B.S. degree in microelectronics from Sichuan University in 2005, and the Ph.D. degree from the Institute of Microelectronics, Chinese Academy of Sciences, in 2010. Her current research interests include MEMS sensors and dielectric film.

Ying Hou received the B.S. degree from the Hebei University of Technology in 2012. She is currently pursuing the Ph.D. degree with the Institute of Microelectronics, Chinese Academy of Sciences.

Chao Liu received the B.S. degree in microelectronics from the University of Electronic Science and Technology of China in 2016, and the M.S. degree from the Institute of Microelectronics, Chinese Academy of Sciences, in 2018, where he is currently pursuing the Ph.D. degree.

Peng Huang received the B.S. degree from Anhui University in 2018. He is currently pursuing the master's degree with the Institute of Microelectronics, Chinese Academy of Sciences.

Dapeng Chen received the M.S. and Ph.D. degrees in physics from the University of Science and Technology of China in 1995 and 1998, respectively. He is dedicated to the research on manufacturing and application of MEMS sensors and multi-sensor integration, especially the research on uncooled infrared focal plane array and its systems.